VTT Technical Research Centre of Finland

Prediction of effective wake at model and Full Scale using a RANS code with an actuator disk model

Sanchez Caja, Antonio; Pylkkänen, Jaakko V.

Published in:
2nd International Conference on Maritime Research and Transportation (ICMRT)

Published: 01/06/2007

Document Version
Publisher's final version

2nd International Conference on Maritime Research and Transportation
Ischia, Italy, 28-30 June 2007

PREDICTION OF EFFECTIVE WAKE AT MODEL AND FULL SCALE USING A RANS CODE WITH AN ACTUATOR DISK MODEL

Antonio Sánchez-Caja and JaakkoV. Pylkkänen
VTT Technical Research Center of Finland

SUMMARY

This paper describes how the effective wake due to the interaction of hull and propeller is estimated using an actuator disk model. The model takes into account the accelerations induced by the propeller in the flow via body forces. The propeller loading is calculated in an interactive way from the propeller geometry using a lifting line off-design model with a pitch-reduction feature for the tip vortices shed from the blades. The paper shows results obtained from applying the model to a fishing vessel. The influence of the free surface on the effective wake is accounted for. Details of the grid at the location of the actuator disk are illustrated. The computational results include a description of the velocity field at the location of the propulsion unit and wave contours generated by the ship hull and the propulsor. The effect of the working propeller on the development of the stern wave is depicted. Scale effects on the effective wake are shown. The effective wake is illustrated in the form of a spatial wake distribution, and quantified in terms of an average volumetric wake fraction. This investigation was part of the EU project SUPERPROP.

1. INTRODUCTION

Within EU Project SUPERPROP, fishing vessels are being studied to improve their operational costs. The optimization of fishing vessels from a propulsive standpoint is not an easy task. Detailed knowledge of the flow at the propeller location and in particular, of the hull wake is needed at the design points. Generally, the operational profile of fishing vessels includes two distinct operating conditions. In free running, the vessels need a relatively high speed to reach the fisheries in a short time. In trawling, they operate at low speed with the nets filled with fish and with propellers developing large thrust. Ducted propellers are suitable for meeting the latter condition efficiently. Usually the design point is selected as a compromise between the two situations.

An important factor to be considered for reducing operational costs is the propeller efficiency, which deteriorates with time as a consequence of the increase of roughness on both propeller and hull. The propeller efficiency should be optimized at the design stage as well as during the operational life of the propeller; sometimes by re-machining the geometry to accommodate it to the new operating conditions.

One of the key issues for an optimum propeller design is the correct estimation of the effective wake resulting from propeller-hull interaction. Notionally, the propeller flow at the location of the propeller consist of three components: the flow as altered by the ship hull in the absence of the propeller (i.e. nominal wake), the propeller induced velocities and the interaction between the two preceding flows. This interaction wake is the result of changes not only in boundary layer thickness (or more generally in spatial distribution of vorticity) but also in wave patterns, which may modify the velocity field at the propeller plane, etc. The effective wake is defined as the sum of the first and third components. The magnitude of scale effects on effective wake is largely dependent on the shape of the ship stern.

Traditionally model scale experiments have been the basis for the estimation of the effective wake in an average volumetric sense. Sometimes the effective wake as obtained from model tests has been assumed to remain valid at full scale. Alternatively, some simple formulae have been developed for its extrapolation to full scale (for example, those recommended by the International Towing Tank Conference).

Over the last years with the advance in RANS equation methods a clear tendency is seen to rely more and more on numerical methods for ship design evaluation. In particular, more insight has been gained in understanding better propeller-hull interaction either by direct modeling of the propeller geometry or by a simplified modeling based on actuator disk theory. Similarly, scale effects on hull and propellers have been also evaluated by RANS codes.

The simulation of the effective wake by RANS methods has been treated in the literature mainly by actuator disk models. Most of these models rely on body forces constant in time (Lobatchev et al, 2001). Some others modify the strength of the body forces as the computation proceed on the basis of the updated

incoming flow in an interactive way (Kerwin et al., 1994; Choi et al., 2001). In this paper an off-design lifting line method is interactively combined with a RANS solver to predict the effective wake. From the lifting line code axisymmetric body forces are introduced into the RANS solver. In turn, from the RANS solver an effective wake field is derived by subtracting from the total velocities the axisymmetric component of the propeller induced velocity. The lifting line calculation is integrated into the RANS solver so that the iterative process is made only once within each iteration of the RANS solver. The very short CPU time required by the lifting line subroutine does not increase noticeably the overall computational time of the RANS solver.

2. NUMERICAL METHOD

2.1 FINFLO SOLVER

The flow simulation in FINFLO is based on the solution of the RANS equations by the pseudo-compressibility method. FINFLO solves the RANS equations by a finite volume method. The solution is extended to the wall and is based on approximately factorized time-integration with local time-stepping. The code uses either Roe's flux-difference splitting or Van Leer's flux-vector splitting for compressible flows and an upwind-based scheme for in-compressible flows. In the latter case, the pressure is center-differenced and a damping term is added via a convective velocity. A multigrid method is used for the acceleration of convergence. Solutions in coarse grid levels are used as starting point for the calculation in order to accelerate convergence. A detailed description of the numerical method including discretization of the governing equations, solution algorithm, etc. can be found in Sanchez-Caja et al. (1999 and 2000). Baldwin-Lomax turbulence model was used in the calculation. Other turbulence models are available and will be tested in the future.

2.2 BOUNDARY TREATMENT

For the calculation of the effective wake free stream pressure, uniform flow and flat free surface are set as initial conditions. Other boundary conditions are as follows.

A free surface boundary condition for wave generation is enforced within a deforming grid technique. On the free surface, three components of the velocities (u, v, w) are extrapolated with zero-gradient normal velocity, i.e.

$$\frac{\partial u}{\partial n} = \frac{\partial v}{\partial n} = \frac{\partial w}{\partial n} = 0$$

The wave equation is evaluated for the wave height h on the actual location of the free surface,

$$\frac{\partial h}{\partial t} + u\frac{\partial h}{\partial x} + v\frac{\partial h}{\partial y} = w$$

The boundary condition for the piezometric pressure is obtained as

$$\varphi = \rho g h$$

On the wetted part of the hull surface, no slip conditions are imposed, and a second order extrapolation is applied for the evaluation of the wall pressure. Uniform flow is specified at the external boundary. The streamwise gradients of the flow variables as well as the pressure difference are set to zero at the propeller outlet block.

In the transom stern region, a dry-transom model is used. The flow is forced to detach from transom edge when the wave height grows above the edge. Other calculations not reported in this paper where made for different trim and sinkage using a wetted transom model.

The computations were performed on Xeon™ 3.06 GHz processors.

2.3 ACTUATOR DISK MODEL

An actuator disk model has been recently developed at VTT and implemented in RANS code FINFLO. The radial distribution of loading on the propeller blade is uniformly spread at each radial station in the circumferential direction and expressed in the form of axial and tangential forces per unit volume. The propeller rake can be easily introduced in the model by adapting the grid shape to the rake line. Only a one-cell layer of body forces is used in the propeller axial direction. This approach allows to obtain the effective wake field directly from the velocity field at the propeller plane, avoiding sophistications in the model that would go beyond the range of accuracy expected in body force simulations. From a practical standpoint, more accurate results would most likely require the inclusion of the real propeller geometry in the RANS calculation.

The actuator disk includes a propeller wake model that accounts for the reduction of hydrodynamic pitch in the vorticity shed from the tip of the propeller blades. For a system of reference rotating with the propeller the flow outside the slipstream has an hydrodynamic pitch angle defined by the axial inflow and the propeller rotational speed. On the other hand, inside the slipstream the axial and tangential propeller induced velocities should additionally be taken into account in calculating the hydrodynamic pitch. The pitch selected for the tip vortex is then determined from the average of the pitches inside and outside the slipstream. The change in pitch at the tip is confined to a transition zone in the radial direction. This approach is inspired in a model presented in Dyne (1993).

The accuracy of the actuator disk approach in estimating the effective wake would depend on the ability of the off-design lifting line method to reproduce

the field of induced velocities generated by the body forces within the RANS code. The approach was tested with the single propeller used in this investigation on an incoming flow equal to unity, i.e. in the absence of hull. The solution for the effective wake in this simple test is the nominal wake, which is equal to one for this particular case. The deviations from the solution are small and are shown in Figure 1. The calculated effective *axial* volumetric wake fraction was -0.0046 for the model with the pitch reduction feature activated at the tip. The exact one is zero.

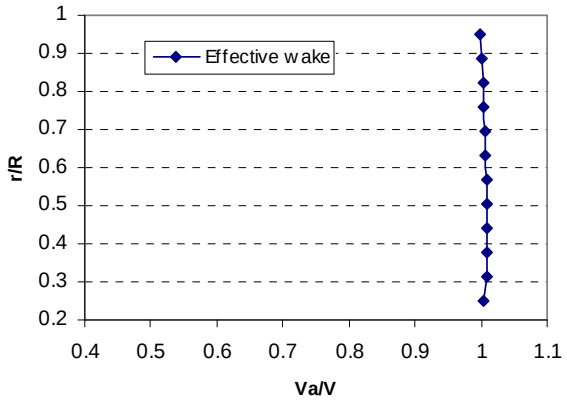

Figure 1. Test of effective wake for a propeller in constant uniform flow. The exact solution is equal to one.

Concerning the tangential and radial effective wake some remarks should be made. Potential flow methods as those based on lifting line theory produce changes in axial and radial velocities that are gradual as the slipstream proceeds in the axial direction. However, the tangential velocity varies abruptly from the location in front of the propeller plane to that behind it, which makes it difficult to define a tangential velocity at the propeller plane. On the contrary, body forces either axial or tangential always produce gradual changes in the velocities. This means that the propeller plane is a suitable place to calculate axial and radial effective wakes, but not the tangential one. Usually the tangential effective wake has not been considered of as much interest as the axial one. For special cases where it is required, a special treatment would be needed for dealing with it.

3. SHIP PARTICULARS AND MESH

The main particulars of the fishing vessel are shown in Table I. The propeller selected for the calculation was a BB series propeller with a similar pitch to that of the fishing boat tested. In principle, the use of a propeller similar to the actual one should be not a major problem for the estimation of the effective wake.

The purpose of the simulation was to find the effective wake for the entire ducted propeller unit. Therefore, the duct and the rudder were not included in the RANS simulation, i.e. the effective wake resulting from the calculations should be considered not for the single propeller but for the propulsor unit (including duct and rudder).

Table I. Fishing vessel. Main particulars.

L_{pp}	67.0 m
$L_{overall}$	77.1 m
B	12.0 m
T	3.6 m
D	7.5 m
Scale	1:12
F_n	0.074-0.262

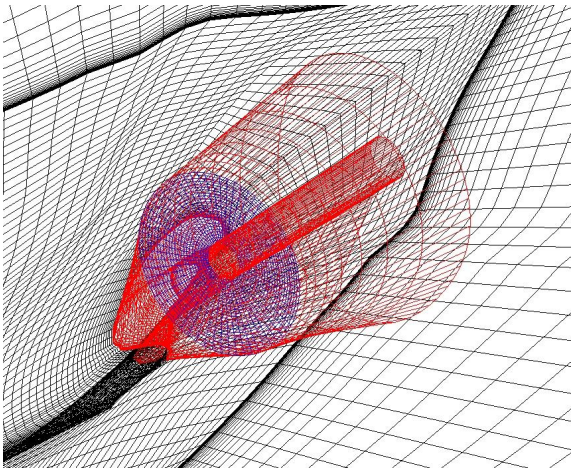

Figure 2. Grid on hull stern and free surface. Detail of actuator disk block. View from beneath.

Table II. Number of cells in the mesh

Free-surface block	Actuator Disk	Total Grid
491,520	196,608	2,162,688

The computational mesh was generated with the IGG grid program and an in-house built program. In order to reduce the number of cells to the maximum extent O-O topology was selected around the hull with a cylindrical block added at the location of the propeller. Both port and starboard sides of the hull were modeled in order to capture the lack of symmetry introduced by the propeller action. The grid deformation was confined to a free-surface block, which has one of its faces coincident with free surface. The grids used in the present calculations consisted of 2.2 million cells distributed in 6 blocks (see Table II). Both model scale and full scale grids have the same number of cells. The stretching near the hull and

the size of the first cell near the wall were modified for the full scale grid relative to the model scale grid, which means that the model scale grid was somewhat over-dimensioned with smaller stretching growth than the full scale grid. The scale factor is l:12. The y+ values were close to one for all calculations. Figure 2 shows a view of the computational mesh at the location of the actuator disk.

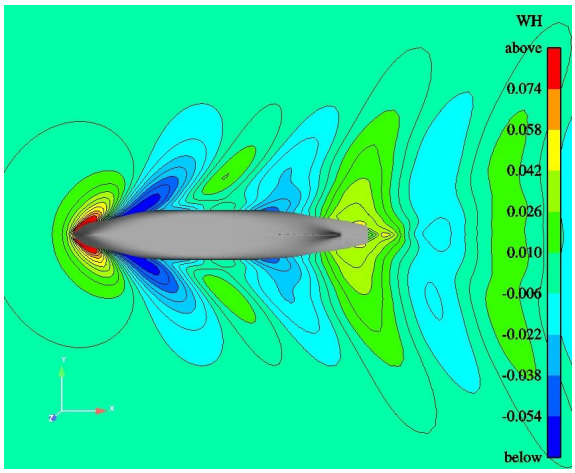

Figure 3. Wave height at 14 knots without propeller action. Model scale. F_n=0.262

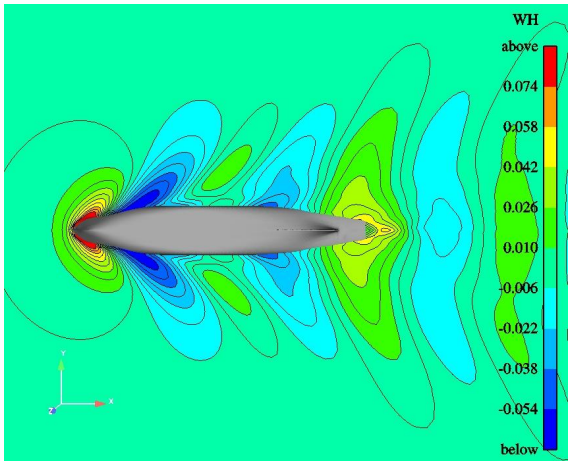

Figure 4. Wave height at 14 knots with propeller action. Model scale. F_n=0.262

3. ANALYSIS OF RESULTS

Calculations were made at the two operating conditions: free running (14 knots) and trawling (4 knots).

3.1 FREE SURFACE

Figures 3 and 4 show an aerial view of the free surface deformation for the model scale calculation at 14 knots for the two cases, i.e. without and with the propeller effects, respectively. The calculation illustrates the growth of the stern wave (in light color) due to the overpressure caused by the propeller action. For the 4-knot case, the wave heights are minimal and therefore no attempt was made to provide a similar comparison. The wave shape was calculated at model scale and assumed to be the same at full scale in order to speed up the calculations. The scaling in the computations was made on a constant Froude number basis.

3.2 PROPELLER PLANE FLOW

Figure 5 shows the axial velocity contours on the propeller plane at model and full scale for the calculations with and without the propeller action at 4 and 14 knots (8 cases in total). The velocities are non-dimensional relative to the ship speed. The propeller location is visible in the figures as a black circular contour.

The velocity field at the propeller plane is noticeably altered by the action of the propeller. The flow is more homogeneous on the propeller plane at full scale. The propeller seems to enlarge the low speed region (0.3) located between the hull and propeller tip at 12 o'clock position for all the cases. On the other hand the speed is considerably increased on the propeller plane.

When comparing the model scale calculations to those at full scale the following features are observed in the flow. A velocity increase in the low speed region (i.e. symmetry plane, up and close to the hull) is shown for the full scale case for the nominal wake, as it is expected. Similarly, for the working propeller condition the low velocity region on top of the propeller is smaller in the full scale calculation. Comparing the non-dimensional results for 4 knots to those for 14 knots at model scale, the main differences are the larger magnitude of the induced velocities due to the stronger velocity deficit at 4 knots. At full scale, a relative stronger wake peak for the 4-knot nominal-wake case is observed in the results at the symmetry plane as compared to the 14 knot ones. However, the average volumetric wake fraction is somewhat larger for the 14 knot case. The reason seems to be a non-physical growth of the wake spatial extent due to excessive turbulent viscosity generated by the algebraic Baldwin-Lomax model.

Figure 6 shows the tangential velocity contours for the same cases. The flow is more accelerated on port side due to the fact that the propeller induced velocity has the same direction as that of the local flow induced by the hull. Somewhat higher tangential velocities are shown for the model scale calculation, which is expected due to the more loaded condition caused by the larger wake fraction. Figure 7 shows the flow direction by velocity vectors for one of the cases in Figure 6 to facilitate the interpretation of this figure.

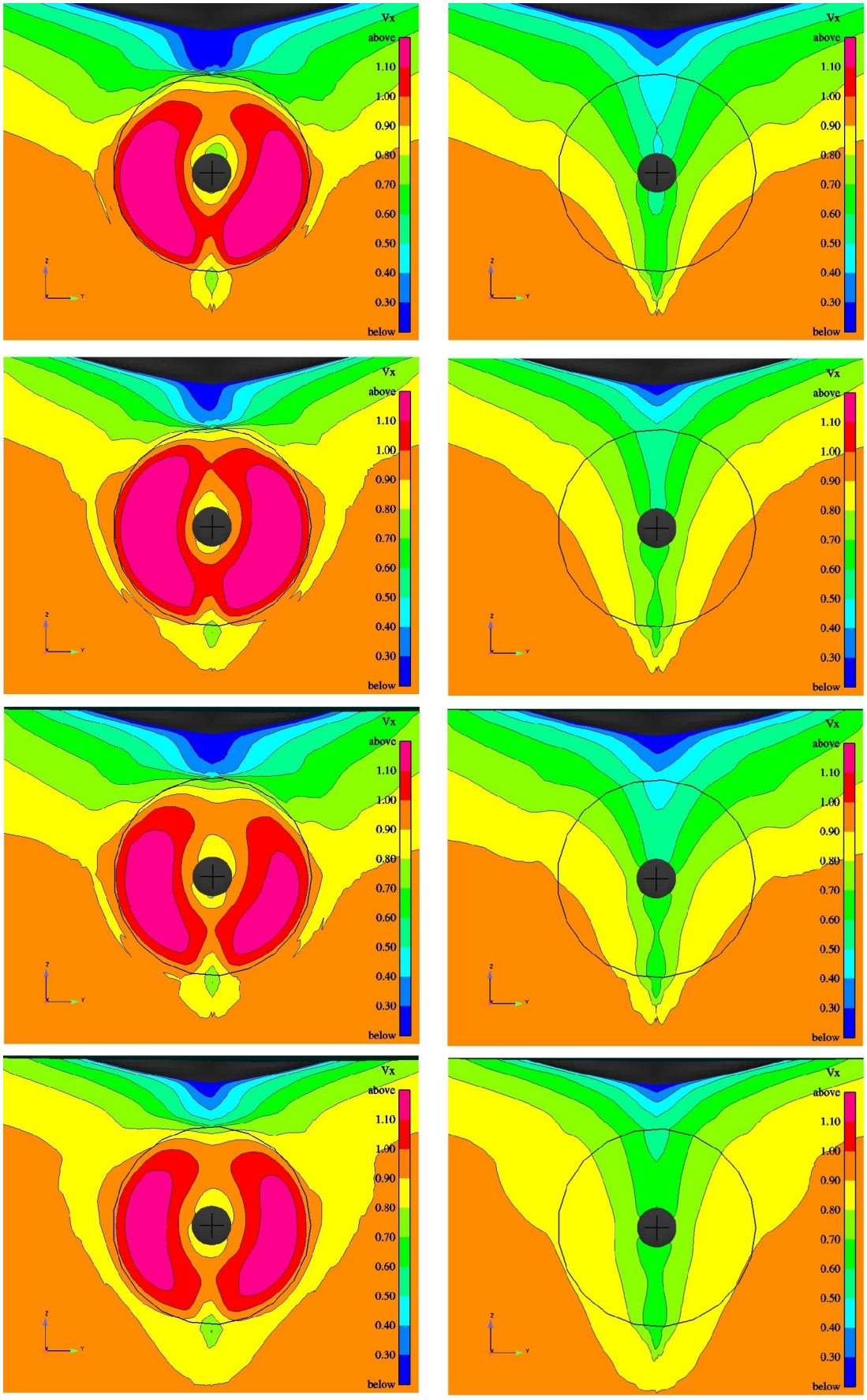

Figure 5. Axial velocity at the propeller plane for the calculation with the propeller action (left) and without (right). From top to bottom: 4 knot model and full scale, 14 knot model and full scale.

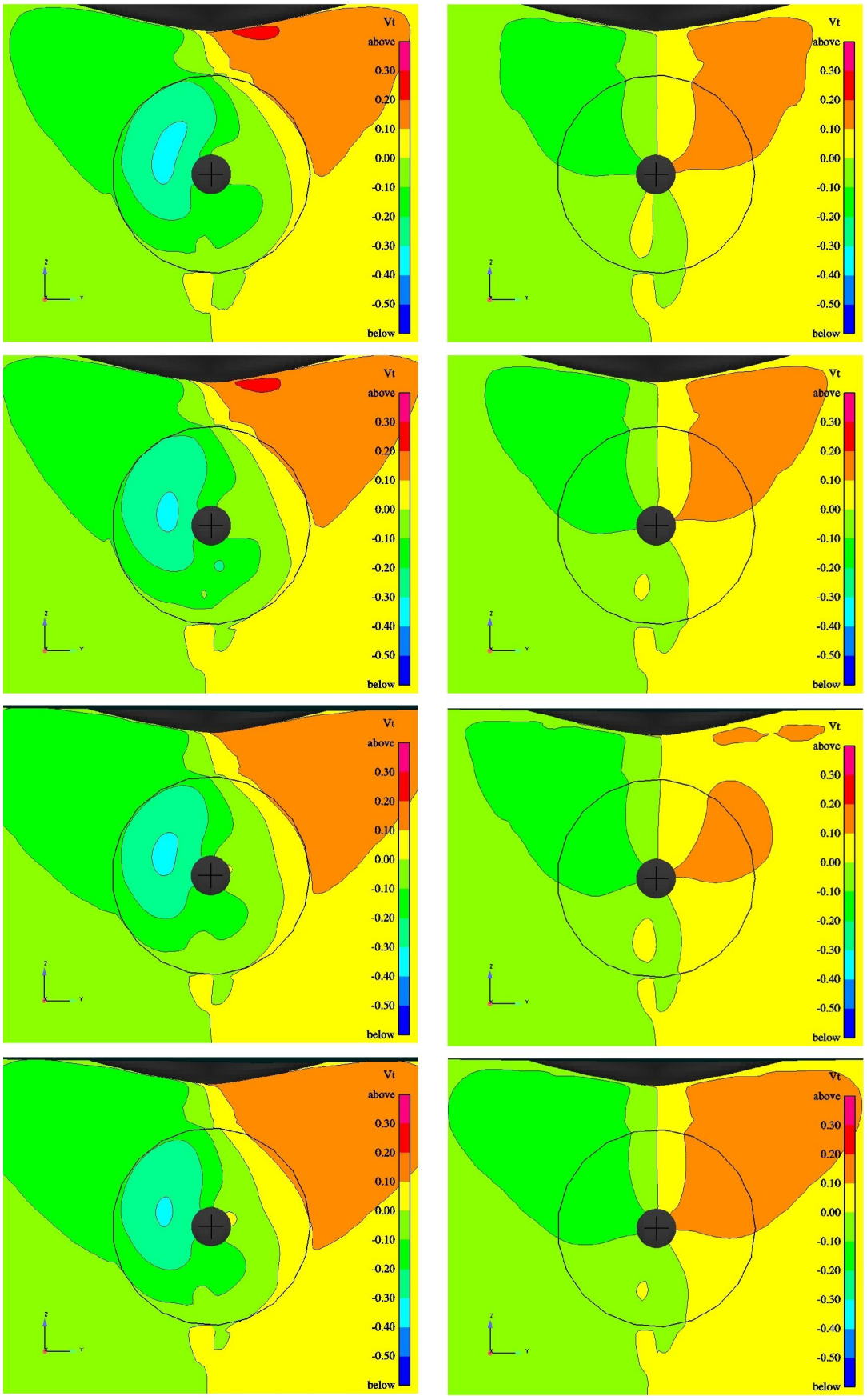

Figure 6. Tangential velocity at the propeller plane for the calculation with propeller action (left) and without (right). From top to bottom: 4 knot model and full scale, 14 knot model and full scale.

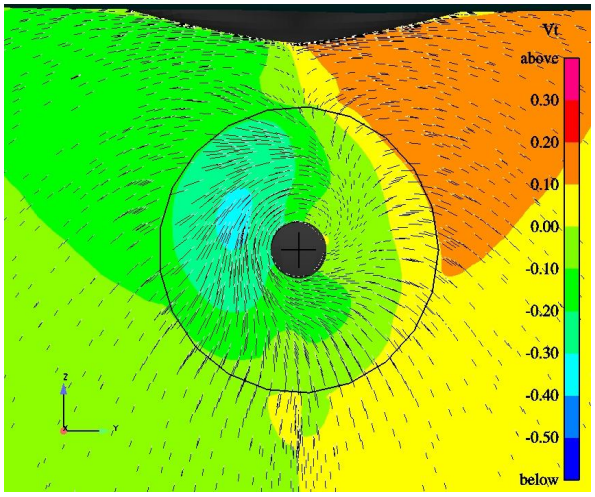

Figure 7. Velocity arrows for interpretation of tangential velocity contours at the propeller.

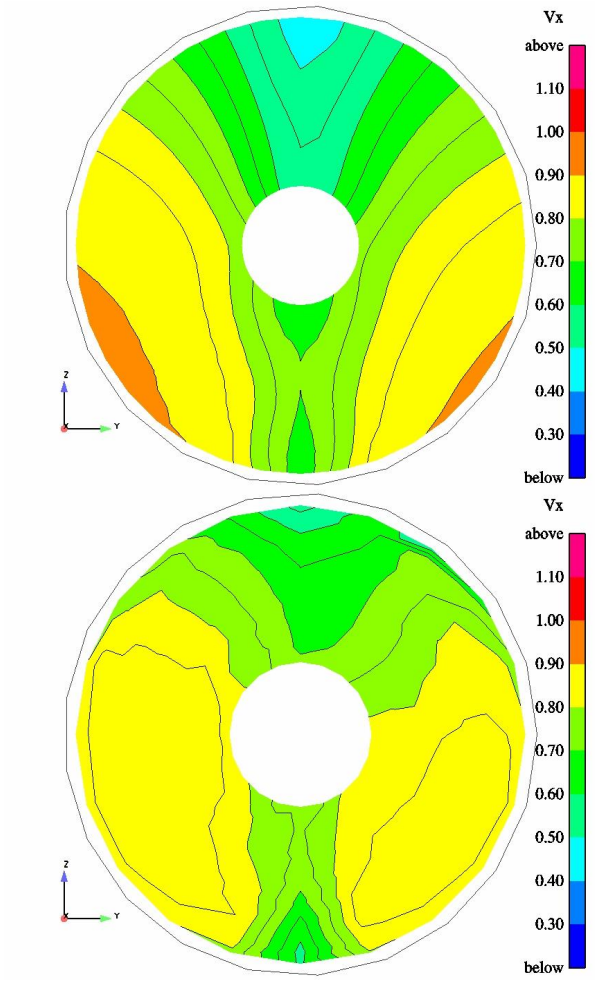

Figure 8. Contours of axial nominal (up) versus effective (down) wake. Model scale. F_n=0.262

3.3 EFFECTIVE WAKE

A summary of the average effective wake calculation is shown in Table III. In principle, the trends in effective wake change are as expected from the standpoint of reduction of wake fraction when passing either from model to full scale or from propelled to un-propelled conditions. The changes in nominal wake from the 4-knot condition to the 14-knot are as expected for the model scale calculations. However, this is not the case at full scale due to deficiencies already mentioned in section 3.2 in Baldwin-Lomax turbulence model.

Table III. Average volumetric axial wake

	knots	Fn	Nominal	Effective
Model scale	14	0.262	0.234	0.209
	4	0.074	0.257	0.229
Full scale	14	0.262	0.216	0.196
	4	0.074	0.206	0.184

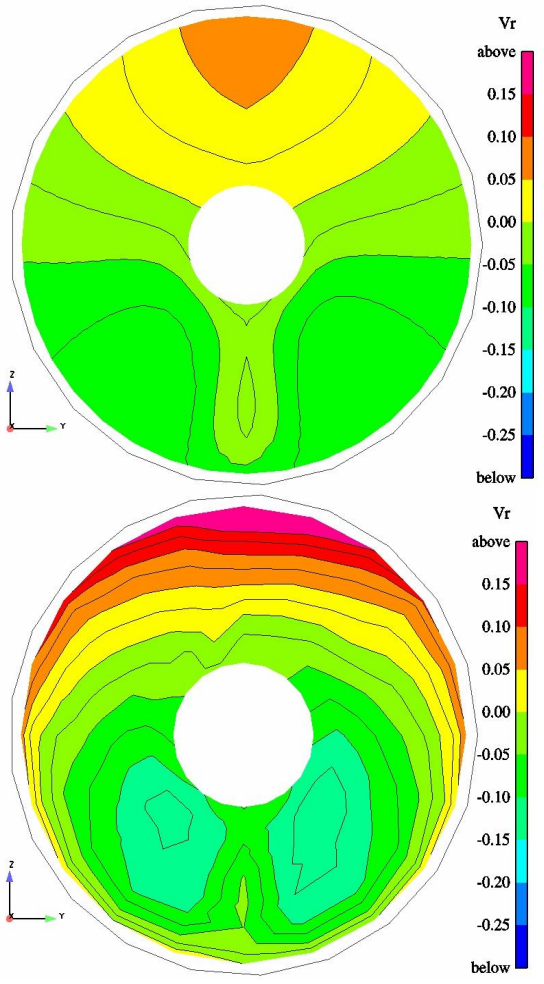

Figure 9. Contours of radial effective wake. Model scale. F_n=0.262

Figure 8 and 9 show the contours of the axial and radial effective wake at model scale, respectively. Positive radial velocity is outwards. The up-wash seen

in the effective radial wake most likely is related to the growth of the stern wave.

4. DISCUSSION

The strong link between nominal wake, effective wake and ship geometry suggests that it is not adequate to start an effective wake calculation from a given nominal wake without reference to the geometry producing such nominal wake, since the interaction with the hull shape is lost. In this work, the actual hull shape geometry was used in the effective wake calculation. It has been illustrated how the effective wake is affected not only by the propeller-induced re-distribution of vorticity in the flow but also by redistributions of pressures affecting for example wave patterns.

Another remark should be made concerning the case of ducted propellers. In section 3 it was said that the effective wake resulting from these calculations is the wake seen not by the isolated propeller, but by the propulsor unit. When trying to estimate the effective wake for a ducted propeller unit, a question arises whether or not to model the thrust provided by the duct by additional body forces.

If we compare the thrust coefficient developed by the duct plus that of the propeller in ducted propeller open water tests, with the thrust coefficient of the same propeller in a propeller open water test (Kawakita, 1992) one can see that the total thrust coefficient could be approximately the same or even somewhat higher for the latter case. This stands for a large range of J values. The reason for this is the acceleration of the flow caused by the duct, which unloads the propeller. The duct thrust compensates to some extent the difference but not all. Therefore, adding additional duct-related body forces with an open propeller actuator disk would not improve the model and could even make it worse. In such a case, the overall thrust loading which is responsible for the magnitude of induced velocities would be overestimated and the simulation would be unbalanced.

A more accurate model would result if the duct geometry is included in the RANS model and the actuator disk is located inside the duct, but in this case the effective wake obtained would be that for the propeller inside the duct not for the duct unit as a whole. The choice of the former or latter model would depend on the approach followed by the ducted propeller designer, i.e. propeller-based or unit-based design.

When using an actuator disk model for effective wake simulation, the order of magnitude in the simplifying assumptions should be kept in mind in order not to unnecessarily complicate the model beyond the range of accuracy expected in body force simulations.

The influence of different turbulence models in the prediction of effective wake will be a topic of future research. The Baldwin-Lomax turbulence model used in the calculations shown in this paper is not very suitable for the present case, especially at full scale.

5. CONCLUSIONS

The incompressible viscous flow around a ship hull has been simulated by solving the RANS equations in combination with an actuator disk model. The FINFLO code was used for the calculations. The grids contained over 2 million cells. Tendencies for flow characteristics in terms of nominal and effective wake at model and full scale are discussed. Wave patterns are shown for the calculations carried out with and without a working propeller at model scale. Some considerations on actuator disk models are made.

ACKNOWLEDGEMENTS

This work has been made within the European Union SUPERPROP project. The authors wish to thank the partners in the SUPERPROP consortium. Special thanks are given to PESCANOVA for providing the geometries subject to investigation.

REFERENCES

Choi, J.K. and Kinnas, S.A., "Prediction of Non-Axisymmetric Effective Wake by a Three-Dimensional Euler Solver," Journal of the Ship Research. Vol. 45, No. 1, March 2001, pp. 13-33.

Kawakita, C., "A Surface Panel Method for Ducted Propellers with New Wake Model Based on Velocity Measurements," Journal of the Society of Naval Architects of Japan. Vol. 172, 1992.

Kerwin, J.E., "A Coupled Viscous/Potential Flow Design Method for Wake-Adapted, Multi-Stage, Ducted Propulsors Using Generalized Geometry," Journal of the Ship Research. Vol. 102, 1994, pp. 23-56.

Lobatchev, M.P., Chicherin, I.A., (2001), "The Full-Scale Resistance Estimation for Podded Propulsion System by RANS Method." Lavrentiev Lectures. Proceeding of International Symposium on Ship Propulsion. SP 2001. 19-21 June 2001, St.Petersburg, pp.39-44.

Sánchez-Caja, A., Rautaheimo, P., Salminen, E., & Siikonen, T., "Computation of the Incompressible Viscous Flow around a Tractor Thruster Using a Sliding Mesh Technique," 7th International Conference in Numerical Ship Hydrodynamics, Nantes (France), 1999.

Sánchez-Caja, A., Rautaheimo, P. and Siikonen, T., "Simulation of Incompressible Viscous Flow Around a Ducted Propeller Using a RANS Equation Solver," 23rd Symposium on Naval Hydrodynamics, Val de Reuil (France), 2000.